JOURNAL OF CATALYSIS **169,** 194–202 (1997)
ARTICLE NO. CA971687

On the Cu Site in ZSM-5 Active in Decomposition of NO: Luminescence, FTIR Study, and Redox Properties

B. Wichterlová,*,[1] J. Dědeček,* Z. Sobalík,* A. Vondrová,* and K. Klier†

*J. Heyrovský Institute of Physical Chemistry, Academy of Sciences of the Czech Republic, CZ-182 23 Prague 8, Czech Republic; and †Lehigh University, Department of Chemistry, Bethlehem, Pennsylvania 18015

Received December 12, 1996; revised February 12, 1997; accepted February 12, 1997

Cu^+ photoluminescence spectra and IR spectra of NO adsorbed on Cu^{2+} in ion exchanged Cu-ZSM-5 of various Cu/Al and Si/Al ratios were employed to identify two main Cu sites (denoted as Cu_α and Cu_β) and their redox properties. The Cu_α site, preferably occupied at low Cu loadings, exhibits more packed environment, higher positive charge, and is proposed to be balanced by two framework Al atoms, while the Cu_β site, occupied in the whole concentration range, but predominantly at high loadings approaching and exceeding 100% degree of ion exchange is in more open coordination, possesses lower positive charge, and is suggested to be balanced by a single framework Al atom. The reducibility of these Cu sites differs substantially and depends on the local negative framework charge, controlled by both the local Si–Al ordering adjacent to the Cu ion and on the total framework charge given by the Si/Al ratio. The correlation of the catalytic activity and reducibility of the Cu-ZSM-5 of various Cu/Al/Si compositions and populations of the Cu_α and Cu_β sites identified the Cu_β site as the active center for NO decomposition. © 1997 Academic Press

INTRODUCTION

Cu ions implanted in ZSM-5 matrices are known to exhibit high and stable activity in the decomposition of NO to molecular nitrogen and oxygen, which has not been attained with these ions embedded in the other zeolite structural types, e.g., in Y and mordenite (1–5). Much effort has been expended to elucidate the mechanism of NO decomposition over Cu-ZSM-5 zeolites, especially over those exhibiting excessively exchanged copper. It is well established that the NO decomposition over Cu-ZSM-5 follows a redox mechanism (6). IR studies of NO adsorbed at room temperature on Cu-ZSM-5 revealed the formation of Cu^+ dinitrosyl species, which were assumed to be precursors of the reaction intermediate (7–9) and monovalent copper to be the active site in the redox process (6). Under the conditions of the catalytic reaction carried out at high temperatures, the surface $Cu(NO)(NO_2)$ complexes were observed (8, 10, 11); however, it has not been proven that these species are real reaction intermediates. Thus, the detailed mechanism of NO decomposition over Cu-ZSM-5 remains unresolved.

There has not been sufficient information on the Cu ion siting and distribution in the high-silica matrices, on the contrary to well-established siting for Cu exchanged into A, X, and Y zeolites (12). Because of the high NO decomposition activity of Cu-ZSM-5 with an overexchanged amount of copper ($Cu/Al > 0.5$), attention has been paid particularly to the zeolites with high Cu loadings. Kucherov and Slinkin (13) reported two coordinations of Cu^{2+} ions in ZSM-5 matrix, square pyramidal and square planar. They suggested that divalent copper can be adjacent to a single framework Al atom as $Cu^{2+}–OH$. Similarly, Kuroda *et al.* (14) found oxygen-bridged Cu^{2+} planar complexes in overexchanged Cu-mordenite. Shpiro *et al.* (15, 16), employing XPS, AES, and XANES suggested the formation of small Cu–O clusters in overexchanged Cu-ZSM-5 zeolites, besides the presence of single Cu ions in ion-exchanged zeolite. Anpo *et al.* (17) employed Cu^+ emission spectra of Cu-ZSM-5 and found two bands at 450 and 540 nm, which they ascribed to monomeric and dimeric Cu^+ species, respectively, analogously to the assignment of Barrie *et al.* (18) for Cu^+ supported on alumina. An EXAFS study (19) produced evidence for the Cu–O distances in Cu-ZSM-5 of 2.01 and 3.13 Å, the latter occurring in the overexchanged zeolites and ascribed to oxidic CuO species.

In connection with the overexchanged Cu-ZSM-5 zeolites, the presence of $(Cu–O–Cu)^{2+}$ bridging species was suggested. Sárkány *et al.* (20, 21) proposed that these species were converted into a pair of Cu^+ cations upon treatment at high temperatures in a stream of helium. On the contrary, Valyon and Hall (11) considered association of extralattice oxygen only with one copper ion in overexchanged zeolites on the basis of IR studies. Larsen *et al.* (22) assumed that $Cu^{2+}O^-$ moieties were formed by dehydration of $(Cu^{2+}–OH)^+$ ions and suggested that the $Cu^{2+}O^-$ and Cu^+ ions were responsible for the Cu-zeolite activity in NO decomposition. Although various Cu species, single

---

[1] Corresponding author. E-mail: wichterl@jh-inst.cas.cz.

0021-9517/97 $25.00

Cu ions, $\mathrm{Cu^+}$ dimers, and Cu–O clusters were suggested, and some of them found in the ZSM-5 matrix, there is no straightforward evidence for the Cu species which really represents the sites active in the reaction of NO decomposition (5).

Recently, we have reported (23) that the Cu siting-coordination in zeolites can be characterized well by the $\mathrm{Cu^+}$ luminescence spectra. Moreover, the intensity of the $\mathrm{Cu^+}$ luminescence bands corresponding to individual Cu coordinations were in sound agreement with the intensities of the shifted vibration bands of NO molecules adsorbed on the precursor divalent Cu sites (24); these shifts reflected a characteristic degree of electron density transferred from the NO molecule to the divalent Cu and, thus, were a measure of effective charges on the individual $\mathrm{Cu^{2+}}$ sites.

We have also found (24) that the Cu-ZSM-5 zeolites contained two dominant Cu sites, whose coordination was assumed to be affected by the local aluminum arrangement in the zeolite framework: (i) Cu ions with the $\mathrm{Cu^+}$ emission at 480 nm, the IR band of NO adsorbed on $\mathrm{Cu^{2+}}$ at 1912 $\mathrm{cm^{-1}}$, and $\mathrm{Cu^{2+}}$ ESR axially symmetrical and split signal with the parameters of the parallel component $g_{\parallel} = 2.33$, and $A_{\parallel} = 140$–160 G, denoted here as Cu_{α}; (ii) Cu ions with $\mathrm{Cu^+}$ emission at 540 nm, the IR of $\mathrm{Cu^{2+}}$–NO at 1895 $\mathrm{cm^{-1}}$, ESR signal with $g_{\parallel} = 2.27$, and $A_{\parallel} = 170$–180 G, denoted as Cu_{β}. The distribution of these sites in the zeolite matrix depended on the Cu loading and Si/Al framework ratio. The latter Cu ions were present in Cu-ZSM-5 regardless of the Cu concentration, but they prevailed in zeolites with high Si/Al ratio and Cu content approaching and exceeding an exchange degree of 100% (i.e., $\mathrm{Cu/Al} \geq 0.5$). This type of dependence of the relative concentration of different copper species on the Cu/Al and framework Si/Al ratio, supported by quantum chemical calculations of energy minima in the aluminosilicate frameworks as well as experimental evidences on the existence of Al pairing in the framework of high silica zeolites (25–28), and observation that divalent Ni ions could not be fully exchanged in ZSM-5 (29) led us to the suggestion that Cu_{β} species are Cu ions adjacent to a single framework Al atom, while species Cu_{α} are balanced by two framework Al atoms.

On the basis of different distribution of the Cu sites in the ZSM-5 zeolites at various Cu loadings and Si/Al framework ratios, a study has been performed to elucidate the relationship between the Cu siting-coordination and the zeolite activity in NO decomposition. Preliminary study indicated that the active site is connected with the Cu_{β} species reflected in the $\mathrm{Cu^+}$ emission band at 540 nm (30). The present contribution deals with a detailed study of the distribution of Cu sites and activity of Cu-ZSM-5 zeolites differing in the Si/Al ratio and Cu loading in a wide range up to Cu overexchange. The Cu active site is proposed and its redox properties are considered in relation to its catalytic activity.

EXPERIMENTAL

Cu-loaded zeolites were prepared by ion exchange of the parent Na-forms of ZSM-5 with diluted aqueous solutions of $\mathrm{Cu^{2+}}$ chloride and $\mathrm{Cu^{2+}}$ acetate. After careful washing the Cu-zeolites were dried in open air to a constant weight. Their chemical compositions are given in Table 1.

The IR spectra of NO adsorbed on Cu-zeolites were monitored on thin transparent plates (ca 7 mg per $\mathrm{cm^{-2}}$) using FTIR spectrometer Nicolet Magna-550 on zeolites treated as given in the figures. $\mathrm{Cu^+}$ luminescence spectra were recorded employing laser (Xe Cl excimer) kinetic nanosecond spectrometer (Applied Photophysics) with the excitation pulse at 308 nm. The spectra of the $\mathrm{Cu^+}$ emission were recorded at 5 μs after the excitation pulse and used for data analysis.

Prior to characterization or catalytic reaction testing the zeolites were treated at 720 K in an oxygen or helium stream or in vacuum. For $\mathrm{Cu^+}$ luminescence measurements the $\mathrm{Cu^{2+}}$ zeolites were reduced by hydrogen as it provided a rather comparable degree of reduction for the individual Cu ions to $\mathrm{Cu^+}$. Figure 1 illustrates the dependence of the intensity of the $\mathrm{Cu^+}$ luminescence bands (reflected individual Cu sites; see below) on the reduction time in hydrogen monitoring the $\mathrm{Cu^{2+}}$–$\mathrm{Cu^{+}}$–$\mathrm{Cu^0}$ reduction process. The emission spectra considered for estimation of the population of the individual Cu sites were recorded on Cu-zeolites reduced in hydrogen at such temperatures at which maximum plateaux of the individual $\mathrm{Cu^+}$ luminescence bands overlapped (see shadow area in Fig. 1). In this region 90% of the Cu ions was reduced to $\mathrm{Cu^+}$ as was verified by a comparison of the intensity of UV-VIS spectra of $\mathrm{Cu^{2+}}$ ions.

Catalytic activity of Cu-zeolites for NO decomposition was determined in a flow-through reactor at 670 K with

TABLE 1

Chemical Composition of CuNa-ZSM-5 Zeolites and Their Catalytic Activity

Si/Al	Cu/Al	Cu (wt%)	TOF[a]
14.1	0.20	1.26	0.6
14.1	0.18	1.10	1.2
14.1	0.33	2.03	3.7
14.1	0.31	1.86	3.9
14.1	0.33	2.03	4.1
14.1	0.41	2.23	5.0
14.1	0.37	2.47	5.5
14.1	0.52	3.05	7.2
14.1	0.56	3.37	6.5
14.1	0.63	3.93	7.1
22.5	0.26	1.10	5.6
22.5	0.23	0.97	6.1
22.5	0.48	1.84	11.2
22.5	0.51	2.00	12.1

[a] NO molecules converted per Cu atom per hour.

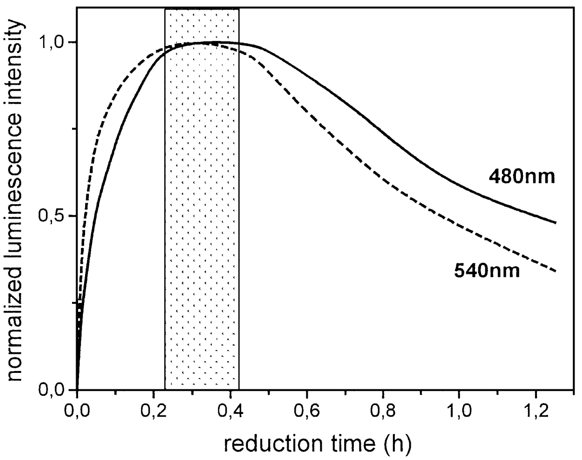

FIG. 1. Dependence of the Cu$^+$ luminescence intensity of the 480 and 540 nm bands on the reduction time. Spectra were recorded at 5 μs. Cu-ZSM-5, Si/Al 22.5, Cu/Al 0.25 reduced in H_2 of 7.5 Torr at 573 K. Intensities were normalized.

typical catalyst weight of about 200 mg containing 3.50 mg of Cu, and helium flow rate of 100 ml/min with inlet NO concentration of 4000 ppm. The reaction product composition was analyzed employing chemiluminescence NO/NOx analyzer (Vamet, CZ); no NO_2 was found within the detection limit 5 ppm. The NO conversions did not exceed 20%.

RESULTS

Figure 2 depicts the Cu$^+$ emission spectra of Cu-ZSM-5 zeolites with different Cu loadings and Si/Al ratios. The intensities of the main bands at 480 and 540 nm differ dramatically in dependence on the Cu-ZSM-5 composition. An additional low intensity band at 450 nm levels off at very low Cu loadings and, thus, the corresponding Cu sites did not reach significant concentrations in any of the studied Cu-ZSM-5 zeolites. Another band of very low intensity, having comparable intensity in all the zeolites investigated here, is observed at 605 nm. It corresponds to trace amounts of Cu ions bonded via terminal Si–OH groups (see Ref. (23)). Because of the very low concentration of both these ions (reflected in Cu$^+$ emissions at 450 and 605 nm) they were not considered in the evaluation of the NO decomposition activity of the Cu sites in the zeolites.

It is clearly seen from Fig. 2 that the Cu ions of type Cu$_\alpha$ (480 nm) dominate at lower Cu loadings and in the zeolites

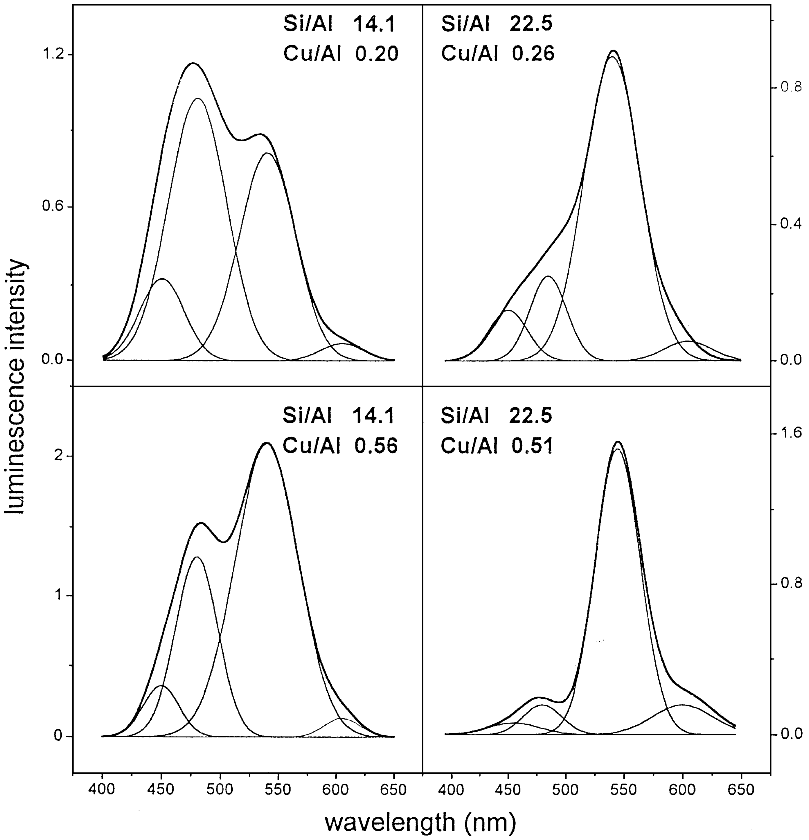

FIG. 2. Cu$^+$ emission spectra of Cu$^+$-ZSM-5 zeolites. Cu-ZSM-5, Si/Al 14.1, Cu/Al 0.20 reduced in H_2 of 7.5 Torr at 473 K for 10 min; Cu-ZSM-5, Si/Al 14.1, Cu/Al 0.56 reduced in H_2 of 7.5 Torr at 473 K for 1.5 min; Cu-ZSM-5, Si/Al 22.5, Cu/Al 0.26 reduced in H_2 of 7.5 Torr at 523 K for 2 min; Cu-ZSM-5, Si/Al 22.5, Cu/Al 0.51 reduced in H_2 of 7.5 Torr at 523 K for 1 min. Spectra were recorded at 5 μs.

with lower Si/Al ratios. On the other hand, in zeolites exhibiting a higher Si/Al ratio and particularly in those with the highest Cu loadings, the Cu sites type Cu_{β} (emission at 540 nm) predominate. A model wherein the 480 nm emission was attributed to Cu^+ bonded via framework oxygens to the "aluminum pairs" (Al–O–(Si–O)$_n$–Al), where we do not specify a value of *n*, but expecting that two Al atoms are as close to copper cation to balance one divalent Cu ion, while the 540 nm emission was due to Cu^+ adjacent to a single aluminum T atom, was put forward in our recent papers (23, 24, 30). It was based on the following assumption on the distribution of the Al atoms in the zeolite framework: at higher Si/Al ratios, a higher number of single framework Al atoms are present in the lattice compared to those possessing a lower Si/Al ratio, where the presence of more "Al pairs" relevant for balancing divalent cations can be expected. The framework Si–Al sequences (far remote single Al atoms and "Al pairs") can affect the Cu ion environment by their electrostatic fields and by different charges on the bridging oxygens (Cu–O–Al) and thus can play an important role in the Cu site binding and chemistry.

However, a distribution of Al in the zeolite framework is not established. A nonrandom distribution of Al in high silica framework of ZSM-5 was suggested at T2 and T12 sites by the calculated energy minima for various Al and Si occupations at T sites (25). But the low population of Al–O–Si–O–Al ordering in the framework of high silica zeolites was indicated by Monte Carlo calculations, considering statistically random distribution of framework Al and Loewenstein rule (26). The existence, but low number, of such type of framework Al pairs was observed also by ^{29}Si MAS NMR for ZSM-5 (28) and ferrierite (31). However, as given above, the "Al pairs" relevant to Cu^{2+} bonding are not restricted to $n = 1$, but also other Si–Al ordering with $n > 1$ should be considered. The number of such "Al pairs" is much higher compared to (Al–O–Si–O–Al) entities, but only the latter pairs can be detected by ^{29}Si MAS NMR and were included in models for quantum chemical calculations.

Lifetimes of the lowest excited states of centers emitted at 480 and 540 nm were 55 and 120 μs, respectively (23, 24). As the ratio of the decay times of the individual emissions calculated using the Einstein coefficients of spontaneous emission is close to the experimental value, and the results of Klier *et al.* for Cu^+–Y zeolite (32) indicate close values of absorption coefficients at wavelengths longer than 300 nm; the quantum efficiency of both centers can be supposed to be similar. In this work, the intensities of the individual bands recored at a decay time of 5 μs were compared with the corresponding integrated intensities of the emissions calculated over the whole emission time. The ratio of the band intensities of the 480 to 540 nm emissions measured at 5 μs with that of the integrated emission intensities from $t = 0$ to ∞ were in agreement within 5%. Therefore, the intensitites of the individual bands as obtained by band separation of the spectra measured at 5 μs and related to the total emission intensity were taken as a measure of the concentration of the individual Cu sites in the sample. Figure 3 depicts the concentration dependence of the Cu sites in ZSM-5 (Si/Al 14.1) reflected in the Cu^+ emission at 480 and 540 nm on the Cu loading in the zeolite.

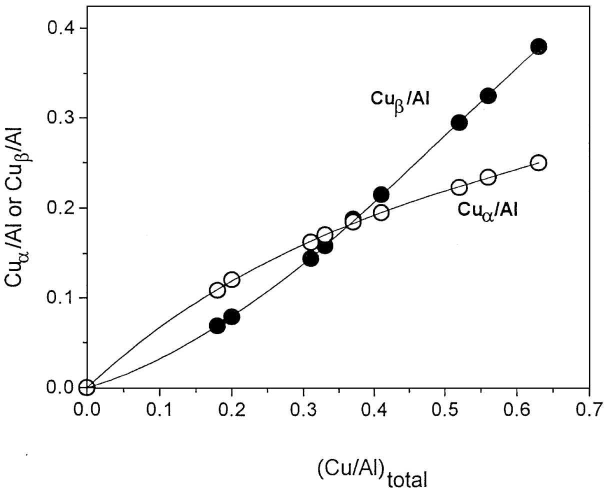

FIG. 3. The dependence of Cu_{α}/Al and Cu_{β}/Al concentration on the total Cu/Al concentration in Cu-ZSM-5 with Si/Al 14.1.

IR spectra of NO adsorbed on Cu-ZSM-5 are shown in Fig. 4. When all the Cu ions were in the divalent state, the spectrum reflects a single broad maximum centered around 1910 cm^{-1} as found also by other authors (7, 10, 11). We have shown (24) that this band consists of two main bands at 1895 and 1912 cm^{-1}, accompanied by a smaller band at about 1921 cm^{-1}. An additional very low intensity band at 1906 cm^{-1} was suggested by the second derivation mode of the IR spectra for Cu-ZSM-5 samples at high Cu loading (not shown in Fig. 4). The intensities of these characteristic IR bands changed with the Cu loading and framework Si/Al ratio parallel to those of the individual Cu^+ emissions; the IR band of adsorbed NO at 1895 cm^{-1} corresponded to the Cu^+ emission at 540 nm and the IR band at 1912 cm^{-1} to the 480 nm emission. Thus, two main Cu sites differing in the degree of electron density, which is transferred from the NO molecule to the divalent Cu ion, have been indicated by the IR spectra of NO adsorbed on the divalent copper. For an estimate of the concentration of the individual Cu sites reflected in various vibrations of adsorbed NO, we assumed identical values for their absorption coefficients. Then the ratio of the integrated intensities of the bands at 1895 and 1912 cm^{-1} was in a sound agreement with the ratio of the intensities of the corresponding 540 and 480 nm Cu^+ bands determined as described above (see Fig. 3).

Figure 5 depicts the IR spectra of NO adsorbed on Cu-ZSM-5 fully oxidized (Fig. 5A, with only Cu^{2+}–NO species present) and partially reduced (Fig. 5B, with both Cu^{2+}–NO

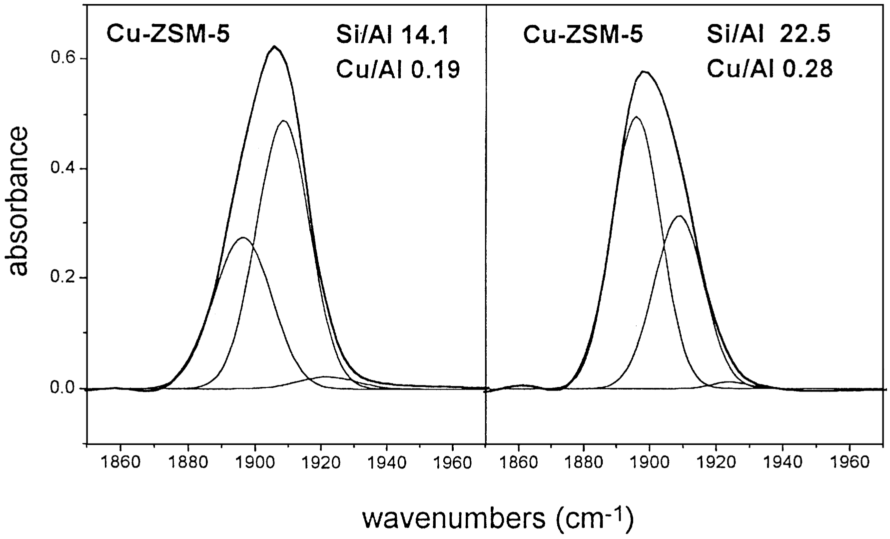

FIG. 4. IR bands of nitrosyl species present on Cu^{2+}-ZSM-5 at 45 Torr of NO; IR spectra measured after NO adsorption at 523 K for 20 min. Spectra were recorded at room temperature.

and Cu^{+}–NO). The presence of the Cu^{+} adsorption centers is clearly seen from the presence of mono and dinitrosyl Cu^{+} complexes with the characteristic bands at 1812, and at 1826 and 1735 cm^{-1}, respectively. From a comparison of the IR spectrum of the completely oxidized Cu-ZSM-5 (Fig. 5A), with that of partly reduced to Cu^{+} (Fig. 5B), it follows that the intensities of the two prominent bands of Cu^{2+}–NO at 1895 cm^{-1} and 1912 cm^{1} differ. As shown also by the difference spectrum (Fig. 5C), the emergence of the Cu^{+}–NO and Cu^{+}–(NO)$_2$ bands is accompanied by the intensity decrease mainly of the band at 1895 cm^{-1}. Thus the Cu sites (IR band at 1895 cm^{-1}) corresponding to Cu$_\beta$ type are readily reduced, compared to the Cu^{2+} ions with NO band at 1912 cm^{-1} corresponding to Cu$_\alpha$ type. The easy reduction of a part of the Cu^{2+} ions in ZSM-5 zeolite was also reported by Larsen *et al.* (22), attributing a partial decrease of the Cu^{2+} ESR signal intensity to the dehydration of the (Cu^{2+}–OH)$^{+}$ exchanged ions and formation of the ESR-silent Cu^{2+}O^{-} species and Cu^{+}. Moreover, we have found that the reducibility of both the Cu sites (Cu$_\alpha$ and Cu$_\beta$) is affected by the total framework Si/Al ratio as documented in Fig. 6. The intensity changes of the Cu^{+} emission bands at 540 nm depending on the reduction time corresponding to the Cu^{2+}–Cu^{+}–Cu^{0} reduction process of the Cu-ZSM-5 zeolites with different Si/Al ratios are presented. The Cu^{2+} ions exchanged into Cu-ZSM-5 with a lower Si/Al framework ratio were not as readily reduced and needed more severe reducing conditions.

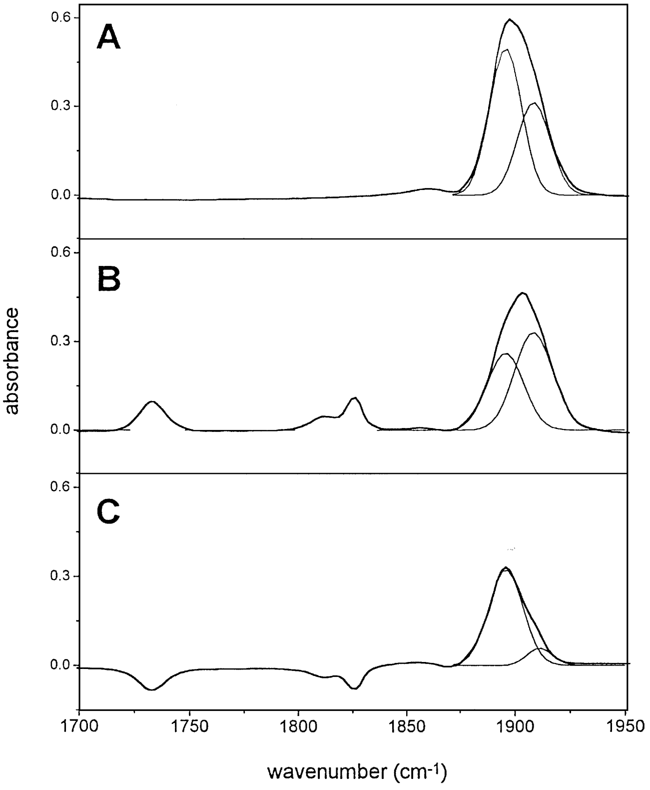

FIG. 5. IR bands of nitrosyl species present on Cu-ZSM-5 (Si/Al 22.5, Cu/Al 0.28) at 45 Torr of NO on fully oxidised (A, adsorption at 523 K) or partially reduced samples via vacuum heat treatment (B, adsorption at 298 K) and the difference spectrum (C) of (A)–(B).

This conclusion on the different reducibility of the Cu ions depending on Cu loading and Si/Al ratio is further supported by our study of CO adsorption on oxidized and on evacuated Cu-ZSM-5 with different Cu/Al and Si/Al compositions (see Ref. (33)). The number of Cu sites reduced under vacuum heat treatment to Cu^{+} is much lower in zeolites with low Cu loadings and low Si/Al, compared to those with high Cu/Al and Si/Al ratios.

The catalytic activity of Cu-ZSM-5 zeolites for NO decomposition was followed in dependence on the

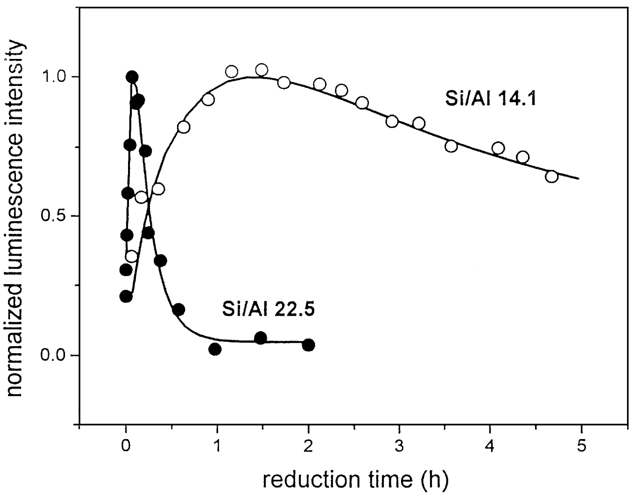

FIG. 6. Dependence of the Cu^+ luminescence intensity of the 540 nm band on the reduction time for zeolites with different Si/Al ratio. Cu-ZSM-5, Cu/Al 0.25 reduced in H_2 of 7.5 Torr at 573 K. Intensities were normalized.

temperature at a constant flow of NO and weight of Cu (3.50 mg) in the tested sample (for details see Ref. (30)). The conversion of NO (NO_2 was not found in the reaction products) increased with increasing temperature, reached a maximum at about 750 K, and then decreased. This pattern of NO conversion with temperature is reversible and typical for the Cu-zeolites and has been ascribed to a reversible change in the reaction kinetics (11). The activity data for all the zeolites are also included in Table 1. Figure 7 depicts a typical relationship between the rate of NO conversion per Cu atom (turnover frequency–TOF is defined as NO molecules decomposed per hour per one Cu atom) depending on the total Cu/Al concentration in the zeolite. The dependence for Cu-ZSM-5 (Si/Al = 14.1) is very similar to that obtained by Valyon and Hall (11). It clearly indicates that the ZSM-5 contains the Cu sites of a higher activity at higher Cu loadings, and moreover, that the Cu sites exchanged into the ZSM-5 matrix with a higher Si/Al ratio (22.5) are more active.

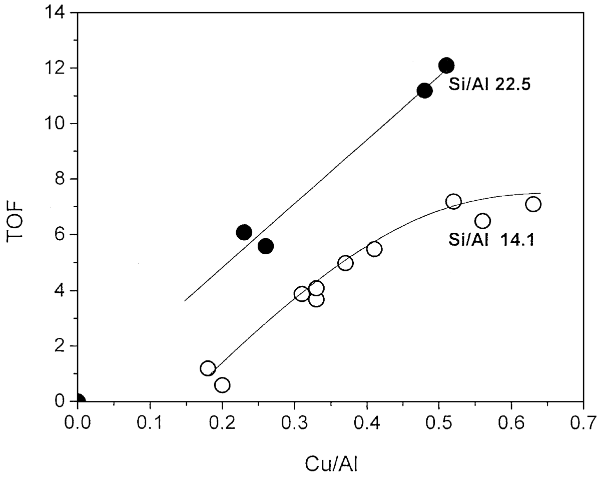

FIG. 7. Effect of Cu/Al and Si/Al ratios in ZSM-5 on the TOF in NO decomposition (NO molecules converted per Cu atom per hour).

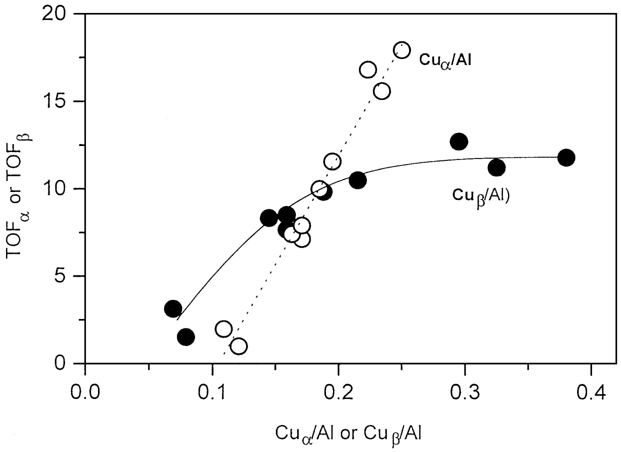

FIG. 8. The dependence of TOF_α and TOF_β corresponding to Cu_α and Cu_β sites, respectively, on the concentration of the individual sites (Cu_α/Al and Cu_β/Al).

An attempt has been made here to differentiate the catalytic activity of the individual Cu sites by using correlation of the rate of NO decomposition with the population of different Cu sites in the ZSM-5 zeolite (Si/Al = 14.1) depending on Cu loading (cf. Figs. 3 and 7). The kinetic data were treated with an assumption that only one type of the Cu site (Cu_α or Cu_β) is the active site, and the contribution of the second one to the total conversion is negligible. Therefore, TOF_α and TOF_β corresponding to the Cu_α and Cu_β sites, respectively, in dependence on the concentration of the individual Cu sites were plotted in Fig. 8. The TOF_α increased dramatically within the whole range of the concentration of the Cu_α sites, while the Cu_β sites exhibit nearly a constant TOF_β value at higher Cu loadings above a value of $Cu_\beta/Al = 0.15$; i.e., Cu_{total}/Al ca 0.3.

DISCUSSION

In order to understand the different wavelengths of the Cu^+ luminescence in different environments, it is helpful to recall the nature of the photoexcited Cu^+ ($3d^9\,4p/4s$) triplet from which emission takes place as a down-transition to the ground singlet Cu^+ ($3d^{10}$). Because of the large radius of the $n = 4$ electron orbital (1.6 Å according to Slater's rules), repulsion of the $4p/4s$ electron by the surrounding lattice will increase the energy of the emitting state and correspondingly will shorten the wavelength of the Cu^+ photoluminescence. This simple model put forward by Texter *et al.* (34) is corroborated by systematic changes of photoemission wavelength from the shortest in highly packed host lattices (e.g., 245 nm in lithium iodide) to long ones (450–600 nm) in open lattices such as zeolites (32, 34, 35).

In regard to the presently studied Cu centers in zeolite matrices, their compositional and structural features, repulsion and other effects can affect photoemission wavelength λ_e as follows:

(i) Electrostatic field generated by nearest negative charge originated from the Al in the T position will give rise to shorter λ_e than that due to nearest Si atoms. Two Al neighbours to the Cu ion will result in shorter λ_e of Cu^+ luminescence than one Al neighbour;

(ii) The open Cu^+ site coordination will give rise to longest λ_e, the recessed and highly coordinated Cu^+ ions will emit at shortest λ_e;

(iii) Dynamic Jahn–Teller effect in the excited Cu^+ triplet is expected to be strong due to a hole in the 3*d* shell. If the site is near planar tri- or penta-coordinated, the effect will be similar to the tri-coordinated Cu^{2+} centers as in Ref. (36) (Jahn–Teller splitting 900 cm^{-1}) and longer luminescence wavelength will ensue. Here we view the excited Cu^+ ions as Cu^{2+} with an extra 4*p*/4*s* electron.

(iv) In previous studies (35, 36) the Cu^+ luminescence wavelength did not depend on whether these ions originated by reduction of Cu^{2+} or by ion exchange of NaY with Cu^+ iodide without reduction. There were also no differences in Cu^+ luminescence wavelengths for CuH- and CuNa-ZSM-5, and for Cu zeolites reduced by hydrogen or CO (37). Therefore the surface protons and oxygen vacancies were ruled out as defects influencing the spectral characteristics of the Cu^+ ions.

As the different Cu^+ luminescence wavelengths at 450, 480, 510, 540 nm are found for Cu ions planted in various zeolite structural types (24, 32) as well as with Cu^+ supported on alumina (18), the wavelength value seems to be dominated by the geometry of the metal ion environment. This supports mechanism given above ad (ii) and (iii).

That the longer wavelength (540 nm) of Cu^+ luminescence in ZSM-5 is associated with an open Cu coordination is also supported by a semiquantitative agreement between the intensity of the Cu^+ luminescence at 540 nm and the intensity of the parallel component of the axially symmetrical Cu^{2+} ESR signal with $g_\parallel$ 2.27 and $A_\parallel$ 170–180 G (24), which was ascribed to Cu^{2+} in a close to planar environment (13). A low degree of electron density transfer from the NO molecule to this Cu_β ion (IR band of NO at 1895 compared to 1875 cm^{-1} for a gaseous NO) reflects a low positive charge on the Cu site, which is in agreement with the assumption that the Cu_β site is balanced by a single Al framework atom, thus by a low negative charge. As already mentioned the distribution of Al in the ZSM-5 zeolites is not known, but the quantum chemical calculations indicate a strong preference of incorporation of only one Al atom into certain framework rings in high silica matrices (31), which oxygens can form a site for this Cu_β ion.

On the other hand, the intensity changes with the Cu/Al/Si concentrations of the shorter Cu^+ emission band at 480 nm, reflecting more packed environment corresponds to the Cu^{2+} ESR signal intensity changes followed in the parallel component of the signal with $g_\parallel$ 2.33 and $A_\parallel$ 140–150 G, attributed to a pyramidal Cu^{2+} coordination. This Cu_α site exhibits a high positive charge manifested by a high degree of an electron density transfer from the NO molecule to the Cu site (band at 1912 cm^{-1}). It supports the suggestion that this Cu ion is balanced by a high negative framework charge produced by two framework Al atoms adjacent to the cation.

Consideration of all these results and information already published on the characteristic spectral features for Cu ions at the cationic sites for various structural zeolite types (13, 24, 34, 36), provides evidence that both the Cu_α and Cu_β ions are at the cationic sites and cannot be assigned to Cu oxidic species. If Cu oxidic species would be present in the zeolite, which can happen at high Cu overexchange, then Cu^+ emissions are expected with much shorter lifetimes, moreover, at higher wavelengths, in contrast to Cu^+ emissions at 480 and 540 nm for the Cu ions in the zeolite cationic sites.

The finding on the different positive charges on the individual Cu sites is in agreement with their different reducibility as documented by the adsorption of NO and CO (see Ref. (33)) on Cu-ZSM-5 with various Cu/Al/Si compositional ratios treated in vacuum at such conditions that only a part of the Cu ions is reduced to Cu^+ (cf. Fig. 5). It clearly follows that the Cu ions of type Cu_β, emitting at 540 nm (Cu^+) and possessing an IR band of adsorbed NO on Cu^{2+} at 1895 cm^{-1}, exhibit an easier reducibility, which is facilitated by their compensation by a single framework Al atom, compared to the Cu_α type sites manifested by the Cu^+ emission at 480 nm and vibration of adsorbed NO on Cu^{2+} at 1912 cm^{-1}. However, the reducibility of both the Cu_α and Cu_β type ions is in addition affected by the total content of aluminum in the framework (cf. Fig. 6 and Ref. (33)); lower total negative framework charge (higher Si/Al ratio) results in an easier reducibility of the Cu ions. It follows that both the local (adjacent to the Cu ion) and total negative framework charge (given by the Si/Al ratio) contribute to the resulting reducibility of the Cu ions.

Thus two main Cu sites with different populations in the ZSM-5 zeolite matrix, depending on the Cu/Al and Si/Al compositions were identified. They differ in coordinations, positive charges on the cations, as well as in redox properties, controlled by the local and total negative framework charge. As the redox properties of the Cu sites are supposed to play a major role in their catalytic activity in the reaction of NO decomposition, the different reducibility of the individual Cu ions in Cu-ZSM-5 with various Cu/Al/Si compositions was considered as a main factor controlling the rate of NO decomposition.

If monovalent Cu ions are active centers, then their higher concentrations at a given reaction condition can be expected in zeolites with a higher Si/Al ratio. This is in line with the observed higher catalytic activity and reducibility of the Cu ions in Cu-ZSM-5 with Si/Al of 22.5, compared to those in ZSM-5 with Si/Al of 14.1 (cf. Figs. 6 and 7, and Fig. 4 in Ref. (33)). Our finding that the Cu sites located in the ZSM-5 matrix with a higher aluminum content are less active than those in high silica material, agrees with the results published by Iwamoto and Hamada (3), but contradicts conclusions given in a review paper by Morretti (38), claiming higher activity for Cu-ZSM-5 zeolites possessing low Si/Al ratios.

A substantially different reducibility of the Cu_α and Cu_β sites in ZSM-5 (Fig. 5) and their different population depending on Cu/Al ratio, together with a clear indication that the Cu sites of different activity are present in the ZSM-5 zeolite (Fig. 7), led us to an attempt to analyze the kinetic data on NO decomposition over Cu-ZSM-5 with Si/Al of 14.1 by using a simplified model, where only one of the Cu sites is considered to be an active center, while the second one is assumed to contribute not significantly to the catalytic activity of the Cu-zeolite and *vice versa*.

As follows from Fig. 8, in such a model the Cu_α site can hardly be considered as an active site, as the TOF_α values for NO decomposition per Cu_α site increases in the whole concentration range. On the other hand, the “flat” dependence of TOF_β for Cu_β sites at higher Cu loadings ($Cu_{total}/Al > 0.3$, i.e., $Cu_\beta/Al > 0.15$) encourage us to claim that these sites dominate in activity for NO decomposition. This conclusion is strongly supported by the fact that the site of type Cu_β exhibits a substantially higher reducibility compared to the Cu_α site, thus enabling the presence of a monovalent state of copper under the conditions of the decomposition reaction.

It should be also noted that when Cu_β ions in our zeolites were transformed into Cu oxidic entities (e.g., by overheating) a decrease in NO decomposition activity was observed (Refs. (37, 39)). It indicated that these oxidic species do not display such high activity as single Cu_β ions.

CONCLUSIONS

Two main Cu sites differing in coordination, positive charges, reducibility, and catalytic activity in NO decomposition were distinguished in ion exchanged Cu-ZSM-5 of various Si/Al and Cu/Al ratios ranging up to the overexchange level. There are no structural data on detail Si–Al ordering in frameworks of high silica zeolites relevant to the bonding of divalent cations. Nevertheless the dependence of the population of the individual Cu sites and spectral information obtained from the Cu^+ emissions and IR vibrations of NO adsorbed on divalent copper, depending on the zeolite composition (Cu/Al/Si), strongly indicate that the Cu_α site is found in more packed environment of two framework Al atoms producing higher local negative charge in vicinity of the Cu ion and, thus, a higher positive charge on the Cu ion. In more general terms, the longer wavelength (540 nm) of the Cu_β ion and relatively long lifetime (120 um) of the excited triplet luminescence of the Cu^+ ions indicates an open coordination due to smaller repulsion by the nearest neighbouring oxygens (34, 36) and therefore greater accessibility of this site to the reactants. The Cu_β site with more open coordination exhibits a lower positive charge on the Cu cation in agreement with the model proposed in our earlier work (24, 30), where the Cu_β ion is balanced by a single framework Al atom (by a lower negative framework charge).

The structural and compositional features are reflected in the redox properties and catalytic activity of the Cu sites. Both the local negative charge (Si–Al ordering) adjacent to the Cu ion and the total negative charge given by the total Al content in the zeolite framework control the Cu ions reducibility and, thus, also the decomposition activity. The environment of the Cu_β center with a low positive charge and open coordination sphere stabilizes the monovalent state of copper to a high extent. Using the correlation of the population of these sites, with their reducibility and catalytic activity, it is concluded that mostly the Cu_β centers are responsible for NO conversion to molecular nitrogen and oxygen. It is of importance that the highest relative population of the Cu_β has been found in overexchanged zeolites with high silica matrix. It can be inferred that the highest decomposition activity per Cu ion could be predicted for Cu-zeolites with high Cu loading and high Si/Al ratio.

ACKNOWLEDGMENTS

The authors acknowledge the financial support of the U.S.-CZ Program for Science and Technology (Project No. 93050), and the authors from the Heyrovský Institute acknowledge, also, the support by the Grant Agency of the Czech Republic (Project No. 203/1993/1130).

REFERENCES

1. Iwamoto, M., Yokoo, S., Sakai, K., and Kagawa, S., *J. Chem. Soc. Faraday Trans. 1* **77**, 1692 (1981).
2. Iwamoto, M., and Yahiro, H., *Catal. Today* **22**, 5 (1994).
3. Iwamoto, M., and Hamada, H., *Catal. Today* **10**, 57 (1991).
4. Li, Y., and Hall, W. K., *J. Catal.* **129**, 202 (1991).
5. Centi, G., and Perathoner, S., *Appl. Catal. A: General* **132**, 179 (1995).
6. Hall, W. K., and Valyon, J., *Catal. Lett.* **15**, 311 (1992).
7. Giamello, E., Murphy, D., Magnacca, G., Morterra, C., Shioya, Y., Nomura, T., and Anpo, M., *J. Catal.* **136**, 510 (1992).
8. Spoto, G., Bordiga, S., Scarano, D., and Zecchina, A., *Catal. Lett.* **13**, 39 (1992).
9. Wichterlová, B., Dědeček, J., and Tvarůžková, Z., *Stud. Surf. Sci. Catal.* **84**, 1555 (1994).
10. Spoto, G., Zecchina, A., Bordiga, S., Ricchiardi, G., and Martra, G., *Appl. Catal. B: Environmental* **3**, 151 (1994).
11. Valyon, J., and Hall, W. K., *J. Phys. Chem.* **97**, 124 (1993).
12. Schoonheydt, R. A., *Catal. Rev. Sci. Eng.* **35**, 129 (1993).

13. Kucherov, A. V., and Slinkin, A. A., *J. Phys. Chem.* **93**, 864 (1989).
14. Kuroda, Y., Kotani, A., Maeda, H., Moriwaki, H., Morimato, T., and Nagao, M., *J. Chem. Soc. Faraday Trans.* **88**, 1583 (1992).
15. Shpiro, E. S., Gruenert, W., Joyner, R. W., and Baeva, G. N., *Catal. Lett.* **24**, 159 (1994).
16. Shpiro, E. S., Joyner, R. W., Gruenert, W., Hayes, N. W., Siddiqui, M. R. H., and Baeva, G. N., Zeolites and related microporous materials: State of the art 1994, *in* "Stud. Surf. Sci. Catal." (Weitkamp *et al.*, Eds.), Vol. 84, p. 1483 (1994).
17. Anpo, M., Nomura, T., Shioya, Y., Che, M., Murphy, D., and Giamello, E., *in* "Proc. 10th Int. Congr. Catal." (L. Guczi *et al.*, Eds.), p. 2155, Akad. Kiado, Budapest, 1993.
18. Barrie, J. D., Dunn, B., Hollingsworth, G., and Zink, J. I., *J. Phys. Chem.* **93**, 3958 (1989).
19. Hamada, H., Matsubayashi, N., Shimada, H., Kintaichi, Y., Ito, T., and Nishijama, A., *Catal. Lett.* **5**, 189 (1990).
20. Sárkány, J., d'Itri, J. L., and Sachtler, W. M. H., *Catal. Lett.* **16**, 241 (1992).
21. Sárkány, J., and Sachtler, W. H. M., *Zeolites* **14**, 7 (1994).
22. Larsen, S. C., Aylor, A., Bell, A. T., and Reimer, J. A., *J. Phys. Chem.* **98**, 11533 (1994).
23. Dědeček, J., and Wichterlová, B., *J. Phys. Chem.* **98**, 5721 (1994).
24. Dědeček, J., Sobalík, Z., Tvarůžková, Z., Kaucký, D., and Wichterlová, B., *J. Phys. Chem.* **99**, 16324 (1995).
25. Derouane, E. G., and Fripiat, J. G., *Zeolites* **5**, 165 (1985).
26. Levits, P., Blumenfield, A. L., and Fripiat, J. J., *Catal. Lett.* **38**, 11 (1996).
27. den Ouden, C. J. D., Jackson, R. A., Catlow, C. R. A., and Post, M. F. M., *J. Phys. Chem.* **94**, 5286 (1990).
28. Gobbi, G. C., Kennedy, G. J., and Fyfe, C. A., *Chem. Lett.* 1551 (1983).
29. den Ouden, C. J. J., Wielers, A. F. H., Kuipers, H. P. C. E., Vaarkamp, M., Mackay, M., and Post, M. F. M., "Zeolites: Facts, Figures, Future" (P. A. Jacobs and R. A. van Santen, Eds.), *Stud. Surf. Sci. Catal.* Vol. 49B, p. 825, 1989.
30. Wichterlová, B., Dědeček, J., and Vondrová, A., *J. Phys. Chem.* **99**, 1065 (1995).
31. Takaishi, T., Kato, M., and Itabashi, K., *Zeolites* **15**, 21 (1995).
32. Strome, D. H., and Klier, K., *J. Phys. Chem.* **84**, 981 (1980).
33. Wichterlová, B., Sobalík, Z., and Dědeček, J., *Catal. Today*, in press.
34. Texter, J., Strome, D. H., Herman, R. G., and Klier, K., *J. Phys. Chem.* **81**, 333 (1977).
35. Maxwell, I. E., and Drent, E., *J. Catal.* **41**, 412 (1976).
36. Strome, D. H., and Klier, K., *Am. Chem. Soc., Symp. Ser.* **135**, 155 (1980).
37. Dědeček, J., *Ph.D. dissertation*, J. Heyrovský Institute of Physical Chemistry, Academy of Sciences, Prague, 1995.
38. Morretti, G., *Catal. Lett.* **23**, 135 (1994).
39. Dědeček, J., Vondrová, A., and Wichterlová, B., in preparation.